THE JOURNAL OF BIOLOGICAL CHEMISTRY VOL. 289, NO. 8, pp. 4653–4659, February 21, 2014
© 2014 by The American Society for Biochemistry and Molecular Biology, Inc. Published in the U.S.A.

TMPyP4 Porphyrin Distorts RNA G-quadruplex Structures of the Disease-associated r(GGGGCC)*n* Repeat of the *C9orf72* Gene and Blocks Interaction of RNA-binding Proteins*

Received for publication, July 16, 2013, and in revised form, December 24, 2013
Published, JBC Papers in Press, December 26, 2013, DOI 10.1074/jbc.C113.502336

Bita Zamiri[‡], **Kaalak Reddy**[§¶], **Robert B. Macgregor, Jr.**[‡], **and Christopher E. Pearson**[§¶1]

From the [‡]*Graduate Department of Pharmaceutical Sciences, Leslie Dan Faculty of Pharmacy, University of Toronto, Toronto, Ontario M5S 3M2, the* [§]*Program of Genetics and Genome Biology, The Hospital for Sick Children, Toronto, Ontario M5G 1L7, and the* [¶]*Program of Molecular Genetics, University of Toronto, Toronto, Ontario M5S 1A1, Canada*

Background: Amyotrophic lateral sclerosis and frontotemporal dementia are caused by expansion of the *C9orf72* (GGGGCC)*n* repeat, whose RNA can form G-quadruplexes.
Results: r(GGGGCC)*n* G-quadruplex distortion by TMPyP4 ablates interaction of the hnRNPA1 and ASF/SF2 proteins.
Conclusion: G-quadruplexes can be modulated by TMPyP4, which can ablate protein interactions.
Significance: Disruption of secondary structures in the *C9orf72* RNA repeats may be a potential therapeutic avenue.

Certain DNA and RNA sequences can form G-quadruplexes, which can affect genetic instability, promoter activity, RNA splicing, RNA stability, and neurite mRNA localization. Amyotrophic lateral sclerosis and frontotemporal dementia can be caused by expansion of a (GGGGCC)*n* repeat in the *C9orf72* gene. Mutant r(GGGGCC)*n*- and r(GGCCCC)*n*-containing transcripts aggregate in nuclear foci, possibly sequestering repeat-binding proteins such as ASF/SF2 and hnRNPA1, suggesting a toxic RNA pathogenesis, as occurs in myotonic dystrophy. Furthermore, the *C9orf72* repeat RNA was recently demonstrated to undergo the noncanonical repeat-associated non-AUG translation (RAN translation) into pathologic dipeptide repeats in patient brains, a process that is thought to depend upon RNA structure. We previously demonstrated that the r(GGGGCC)*n* RNA forms repeat tract length-dependent G-quadruplex structures that bind the ASF/SF2 protein. Here we show that the cationic porphyrin (5,10,15,20-tetra(*N*-methyl-4-pyridyl) porphyrin (TMPyP4)), which can bind some G-quadruplex-forming sequences, can bind and distort the G-quadruplex formed by r(GGGGCC)8, and this ablates the interaction of either hnRNPA1 or ASF/SF2 with the repeat. These findings provide proof of concept that nucleic acid binding small molecules, such as TMPyP4, can distort the secondary structure of the *C9orf72* repeat, which may beneficially disrupt protein interactions, which may ablate either protein sequestration and/or RAN translation into potentially toxic dipeptides. Disruption of secondary structure formation of the C9*orf*72 RNA repeats may be a viable therapeutic avenue, as well as a means to test the role of RNA structure upon RAN translation.

Amyotrophic lateral sclerosis (ALS),[2] also known as Lou Gehrig disease, and frontotemporal dementia (FTD) are part of a spectrum of neurodegenerative disorders (1). Expansion of a (GGGGCC)·(GGCCCC) hexanucleotide repeat within the first intron of the *C9orf72* gene is one of the most common causes of ALS and FTD (1–3). Unaffected individuals have 2–19 repeats, and individuals with as few as 20–25 repeats may show symptoms of disease, whereas those affected can have 250–2100 repeats (2–4).

Patient cells bearing the expanded repeat contain ribonuclear foci containing the r(GGGGCC)*n* repeat, suggesting a toxic RNA-protein sequestration pathway similar to other repeat expansion diseases (2, 5). In myotonic dystrophy type 1 (DM1), expanded r(CUG)*n* RNAs fold into hairpin structures that are recognized by the muscleblind (MBNL) family of alternative splicing regulators, leading to their binding and sequestration. Loss of muscleblind results in the missplicing of its many downstream mRNA targets, leading to DM1 pathogenesis (5). Several proteins have been identified that bind to the r(GGGGCC)*n* RNA *in vitro* and *in vivo* (6–8), which may influence ALS-FTD pathogenesis through the toxic RNA gain-of function pathway. ASF/SF2 splicing regulator was shown to interact with the r(GGGGCC)*n* repeat *in vitro* (7) and to be present in RNA foci in cells with expanded (GGGGCC)*n* tracts (9). The protein hnRNPA3 selectively binds the r(GGGGCC)*n* repeats *in vitro* and was identified in intracellular inclusions of ALS-FTD patient brains (6). Most recently, the Pur-α protein, which interacts with expanded r(CGG)*n* repeats associated with fragile X-associated tremor ataxia and fragile X premature ovarian insufficiency, was demonstrated to interact with expanded r(GGGGCC)*n* repeats *in vitro* and *in vivo* (in *Drosophila* and FTD patient brain samples), forming intracellular inclusions (8). Overexpression of Pur-α in this *Drosophila* model reversed sequestration-associated toxicity (8). These findings support a toxic RNA-mediated protein sequestration model of ALS-FTD pathogenesis. Interestingly, a recent study

* This work was supported by grants from the Amyotrophic Lateral Sclerosis Association of America (to C. E. P.), the Canadian Institutes of Health Research (CIHR) (to C. E. P.), and the Natural Science and Engineering Research Council of Canada (to R. B. M.).
[1] To whom correspondence should be addressed: Program of Genetics and Genome Biology, The Hospital for Sick Children, 101 College St. East Tower, 15-312 TMDT, Toronto, Ontario M5G 1L7, Canada. Tel.: 416-813-8256; Fax: 416-813-4931; E-mail: cepearson.sickkids@gmail.com.

[2] The abbreviations used are: ALS, amyotrophic lateral sclerosis; FTD, frontotemporal dementia; RAN translation, repeat-associated non-AUG translation; hnRNPA1, heterogeneous nuclear ribonucleoprotein A1; TMPyP4, 5,10,15,20-tetra(*N*-methyl-4-pyridyl) porphyrin; ASF/SF2, alternative splicing factor/splicing factor 2.

This is an open access article under the CC BY license.

identified point mutations in the hnRNPA1 gene resulting in protein aggregation causing ALS-FTD (10). Both hnRNPA1 and hnRNPA3 were identified as r(GGGGCC)*n*-binding proteins, among others (6). The presence of hnRNPA1, hnRNPA3, or any protein at the r(GGGGCC)*n*-positive foci is presently unknown.

The expanded r(GGGGCC)*n* and r(GGCCCC)*n* RNAs can undergo repeat-associated non-AUG (RAN) translation to form aggregating dipeptide repeat inclusions in ALS-FTD patient brains (6, 11–15), a phenomenon initially demonstrated for the myotonic dystrophy type 1 and spinocerebellar ataxia type 8 repeats (16, 17) and more recently by the CGG repeats of fragile X-associated tremor ataxia (10, 14). Some data suggest a role of RNA structures in RAN translation (6, 12, 16).

The structure assumed by the r(GGGGCC)*n* repeats may contribute to its interaction with proteins to mediate protein sequestration and/or RAN translation. To this end, the toxic RNA may serve as a potential therapeutic target to disrupt these potentially toxic downstream processes, as has been demonstrated for the myotonic dystrophy hairpin-forming r(CUG)*n* RNA (18). Secondary structures of the repeat tracts in the RNA appear to be the basis for both protein sequestration and RAN translation. Our group and others recently demonstrated that r(GGGGCC)*n* forms extremely stable G-quadruplex structures (7, 19). G-quadruplex formation by the r(GGGGCC)*n* repeat may affect protein binding, foci formation, and RAN translation (7).

In G-quadruplexes, four guanine residues are hydrogen-bonded to one another via Hoogsteen base interactions, forming a planar complex (G-quartet) (see Fig. 1*A*). These planar G-quartets can stack upon each other in the presence of Na^+ or K^+ and form stable structures known as G-quadruplexes (see Fig. 1*C*) (20–22). G-quadruplexes have been shown to exist in living cells (23, 24). Functionally, G-quadruplex structures in RNA have been implicated in almost all aspects of pre-mRNA and mRNA metabolism including mRNA stability, internal ribosomal entry site-dependent translation initiation, translational repression, alternative splicing, and alternative polyadenylation/3′ end formation, suggesting that the G-quadruplex may be an important regulatory motif. The *C9orf72* gene is one of the 3000 (16%) genes in the human genome to have motifs with the potential to form G-quadruplexes present in their first intron (25). Many transcripts with G-quadruplex-forming motifs are neurologically important, and their G-quadruplexes are thought to be important for transcript localization to neural synapses by the G-quadruplex-binding FMRP protein (26–31).

The cationic 5,10,15,20-tetra(*N*-methyl-4-pyridyl) porphyrin (TMPyP4) (see Fig. 1*B*) has been shown to stabilize many DNA G-quadruplexes (32). In some instances TMPyP4 can destabilize and unfold RNA G-quadruplexes such as the one present in the *MT3-MMP* mRNA (33). Similarly, TMPyP4 destabilized the G-quadruplex of both the DNA and the RNA (CGG)*n* repeats of *FMR1*, associated with premutation expansions of fragile X syndrome, fragile X-associated tremor ataxia, and fragile X premature ovarian insufficiency (34–36). Disruption of both RNA G-quadruplexes (*MT3-MMP* and *FMR1*) by TMPyP4 led to enhanced levels of translation in model systems (33, 35). Here we report the binding of TMPyP4 to the ALS-FTD r(GGGGCC)8 repeat using gel mobility shift assays, CD spectroscopy, and UV spectroscopy. Additionally, we report that TMPyP4 disrupts the binding of ASF/SF2 and hnRNPA1 to the ALS-FTD-associated r(GGGGCC)8 repeat.

EXPERIMENTAL PROCEDURES

RNA Oligonucleotide Synthesis and Labeling—The RNA oligonucleotides, r(GGGGCC)*n*, $n = 2,5,8$, were purchased from Invitrogen. Oligonucleotides were end-labeled using [γ-^{32}P]ATP. RNA concentrations were determined by recording their absorbance at 260 nm using a molar extinction coefficient of 124,280, 310,700, and 497,120 $\text{M}^{-1}\text{cm}^{-1}$, respectively (37). The RNA was dissolved in 100 mM KCl, 10 mM Tris-HCl, and 0.1 mM EDTA (pH 7.5). The samples were heated to 95 °C and allowed to cool to room temperature.

CD Spectroscopy—CD experiments were performed at room temperature (unless otherwise stated) using an Aviv model 62 DS spectropolarimeter using 5 μM RNA samples dissolved in 100 mM KCl, 10 mM Tris-HCl, and 0.1 mM EDTA (pH 7.5). An average of three CD spectra, over the wavelength range of 320–220 nm, was recorded in a 1-mm path length cuvette at a scan rate of 20 nm/min. For the titrations, 1-μl aliquots of 1 M TMPyP4 in the same buffer as the RNA were added to the sample and mixed before recording the spectrum.

Native Gel Electrophoresis—5′ end-labeled r(GGGGCC)8 was annealed as described above. The radiolabeled RNA was incubated with the indicated amounts of TMPyP4, ASF/SF2 (Abcam), and hnRNPA1 (Abcam) for 30 min at room temperature. Each 10-μl sample contained <10 fmol of [γ-^{32}P]ATP end-labeled RNA in 100 mM KCL, 10 mM Tris-HCl (pH 7.5). For protein binding, the buffer contained 10 mM HEPES (pH 7.9), 200 mM KCl, 20 mM NaCl, 0.025% Nonidet, 1 mM DTT, 10% glycerol. After incubation the samples were loaded onto 8% polyacrylamide gel and electrophoresed at 100 V for 1 h in 1× Tris borate-EDTA, at room temperature, dried, and autoradiographed.

Absorption Spectroscopy—Absorption spectra were measured on a Cary model 300 Bio spectrophotometer. The sample was contained in a 1-mm path length cuvette. Aliquots of r(GGGGCC)*n*, $n = 2,5,8$ in buffer were titrated into a 15 μM sample of TMPyP4 (250 μl). The titrations were terminated when the wavelength and intensity of the absorption band for TMPyP4 did not change upon further addition of RNA. All values are corrected for dilution effects.

The concentration of free porphyrin was determined using a molar extinction coefficient of 226,000 $\text{M}^{-1}\text{cm}^{-1}$. The concentrations of free (C_f) and bound porphyrin (C_b) were calculated using $C_f = C(1 - \alpha)$ and $C_b = C - C_f$, respectively, where C is the total TMPyP4 concentration (15 μM). The fraction of bound porphyrin (α) was calculated using the equation $\alpha = (A_f - A)/(A_f - A_b)$, where A_f and A_b are the absorbance of the free and fully bound TMPyP4 at the Soret maximum of the porphyrin, respectively, and A is the absorbance at the Soret maximum of porphyrin at any given point during the titration. The percentage of hypochromicity of the Soret band of porphyrin can be calculated using

$$\%\ \text{of hypochromicity} = \left[\frac{\epsilon_f - \epsilon_b}{\epsilon_f}\right] \times 100 \qquad \text{(Eq. 1)}$$

where $\epsilon_b = A_b/C_b$ (19, 38).

RESULTS AND DISCUSSION

TMPyP4 Binds to the ALS-FTD r(GGGGCC)n Repeat—To determine whether TMPyP4 can interact with the r(GGGGCC)8 RNA, we performed electrophoretic mobility shift assays where radiolabeled r(GGGGCC)8 was preincubated in the presence of 0, 10, 25, 50, and 100 μM TMPyP4. Multiple electrophoretic species are evident for r(GGGGCC)8, representing uni- and multimolecular G-quadruplex structures, as demonstrated previously (Fig. 1*D*, see *first* and *last lanes*) (7). Increasing the concentration of TMPyP4 led to a progressive shift in the RNA where RNA-drug complexes are retained in the well at high drug concentrations (Fig. 1*D*, *lanes 2–5*). At concentrations higher than 25 μM TMPyP4, the intensity of the faster migrating species decreased, whereas the intensity of the slower migrating species did not change considerably.

To further investigate the interaction between TMPyP4 and r(GGGGCC)*n*, we measured the visible absorption titration spectra (Fig. 1*E*). This method can identify RNA-ligand interactions as shown previously for the binding of *MT3-MMP* mRNA to TMPyP4 (33). The r(GGGGCC)8 oligonucleotides were titrated into a solution of TMPyP4, and the Soret band was monitored as a function of RNA concentration (Fig. 1*E*). The hypochromicity seen upon increasing concentration of r(GGGGCC)8 was 64% with a bathochromic shift of 17 nm indicative of the binding of TMPyP4 to r(GGGGCC)8. The data also reveal an apparent isosbestic point at 439 nm. The same analysis was performed on lengths of 2 and 5 repeats with a similar effect (data not shown). The bathochromic shift for r(GGGGCC)2 and r(GGGGCC)5 was recorded as 15 and 16 nm (data not shown). The C-rich *C9orf72* repeat strand, which does not form a quadruplex structure (7), interacted with TMPyP4 with reduced affinity relative to the G-rich strand (data not shown), consistent with a preference of TMPyP4 for G-quadruplexes. Thus, we demonstrate by two independent means that the r(GGGGCC)*n* repeat is able to interact with TMPyP4 in a concentration-dependent manner. A titration of increasing TMPyP4 suggests that the mode of its interaction may not be limited to external stacking at G-quadruplex ends and may involve intercalation between the G-quartets based on the ratio of the titrated TMPyP4 to the ratio of the RNA sample at the point where the binding plot plateaus (Fig. E, *inset*). Other studies suggest a stacking of TMPyP4 on G-quartets (39).

TMPyP4 Induces a Structural Change in the r(GGGGCC)n Repeat—CD spectroscopy is useful for monitoring changes in the secondary structure of nucleic acids, including G-quadruplexes. As shown previously, the CD spectrum of the r(GGGGCC)*n* repeats in potassium chloride exhibits a positive peak around 260 nm and a negative peak around 240 nm (Fig. 1, *F–H*), which are the spectral characteristics of a parallel-stranded G-quadruplex (7, 40, 41). The addition of TMPyP4 to r(GGGGCC)*n* led to the appearance of a shoulder at around 290 nm in addition to the G-quadruplex specific positive peak at 260 nm (Fig. 1, *F–H*). An induction of a 290 nm shoulder in a G-quadruplex detected by CD spectra in the presence of TMPyP4 has previously been reported as the appearance of antiparallel conformations in another G-rich sequence (42). Thus, in the presence of increasing concentrations of TMPyP4, the r(GGGGCC)*n* RNA undergoes a conformational change. At low concentrations of TMPyP4, the intensity of the 260 nm peak increased, and the intensity was highest at 29 μM TMPyP4 to 5 μM r(GGGGCC)$_8$ ratio (data not shown). Higher concentrations of TMPyP4 led to a decrease of the intensity of the peak at 260 nm and no further change at 290 nm (Fig. 1, *F–H*). The decrease in the intensity of the 260 nm band upon increasing the concentration of TMPyP4 may indicate possible unfolding of the r(GGGGCC)*n* G-quadruplex, as reported previously (33). The CD spectra in Fig. 1*F* are consistent with the gel electrophoresis and Soret band shift experiments in Fig. 1, *D* and *E*, respectively. It is important to note that the r(GGGGCC)*n* G-quadruplex is extremely thermostable and remains folded at temperatures as high as 95 °C (7). Thus, TMPyP4 can modulate the extremely stable structure assumed by the r(GGGGCC)*n* repeat.

To assess the stability of the r(GGGGCC)8 G-quadruplex in the presence of TMPyP4, CD spectra were recorded at different temperatures (data not shown). The porphyrin/RNA molar ratio (20 μM TMPyP4 to 5 μM r(GGGGCC)8) was selected where the intensity of the 260 nm band is at its highest and the shoulder around 290 nm is present. The CD spectra were measured at 0, 24, and 48 h after the addition of TMPyP4 to r(GGGGCC)8. The spectra did not vary over this time period. Upon increasing the temperature, the intensity of the shoulder at 295 nm decreased, whereas the intensity of the positive peak at 260 nm did not change (data not shown). At 75 °C the CD spectra resembles the CD spectra of the RNA G-quadruplex in the absence of TMPyP4 (positive peak around 260 nm and negative peak around 240 nm without the shoulder at 290 nm). This is consistent with the previously observed thermostability of the r(GGGGCC)8 G-quadruplex structure (melting temperature higher than 95 °C) (7). Notably, upon lowering the temperature, the CD spectrum was not different from the one recorded at 95 °C (no shoulder appeared around 290 nm) (data not shown), indicating an irreversible melting process. UV melting experiments were also performed in the presence of TMPyP4 (data not shown). The melting temperature of r(GGGGCC)8 with TMPyP4 was 67 °C, and the melting was irreversible, which was consistent between CD and UV melting experiments. The irreversibility of the melting of r(GGGGCC)8 in the presence of TMPyP4 may be related to the molecularity of the porphyrin-induced structure and may indicate the induction of multimeric G-quadruplexes rather than a monomeric one, as reported previously for other G-quadruplex-forming sequences (43). Thus, TMPyP4 lowered the thermal stability of the r(GGGGCC)8.

TMPyP4 Disrupts Binding of ASF/SF2 and hnRNPA1 to r(GGGGCC)8—The interaction between TMPyP4 and the r(GGGGCC)*n* repeat may alter the interaction of proteins, previously shown to bind the r(GGGGCC)*n* repeat (6–9). To test this, we first assessed the binding of ASF/SF2 to r(GGGGCC)8 in the presence of TMPyP4 (Fig. 2*A*). A distinct slower migrating RNA complex was evident in the presence of purified ASF/SF2 protein (Fig. 2*A*, *lane 2*, see *arrowhead*). In the presence of

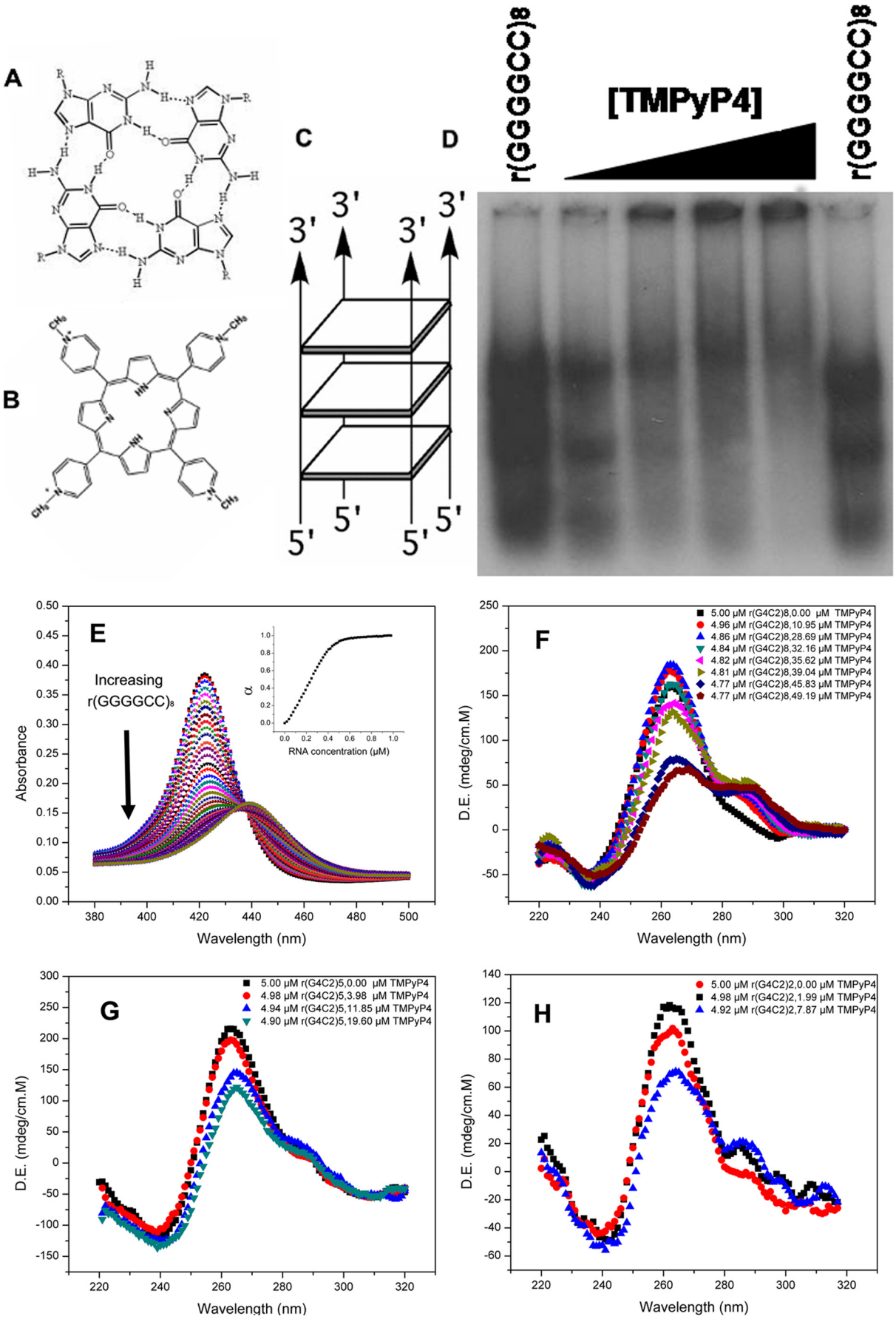
A
B
C
D
3'
5'
r(GGGGCC)8
[TMPyP4]
r(GGGGCC)8
E
Increasing
r(GGGGCC)8
Absorbance
Wavelength (nm)
α
RNA concentration (μM)
F
5.00 μM r(G4C2)8,0.00 μM TMPyP4
4.96 μM r(G4C2)8,10.95 μM TMPyP4
4.86 μM r(G4C2)8,28.69 μM TMPyP4
4.84 μM r(G4C2)8,32.16 μM TMPyP4
4.82 μM r(G4C2)8,35.62 μM TMPyP4
4.81 μM r(G4C2)8,39.04 μM TMPyP4
4.77 μM r(G4C2)8,45.83 μM TMPyP4
4.77 μM r(G4C2)8,49.19 μM TMPyP4
D.E. (mdeg/cm.M)
Wavelength (nm)
G
5.00 μM r(G4C2)5,0.00 μM TMPyP4
4.98 μM r(G4C2)5,3.98 μM TMPyP4
4.94 μM r(G4C2)5,11.85 μM TMPyP4
4.90 μM r(G4C2)5,19.60 μM TMPyP4
D.E. (mdeg/cm.M)
Wavelength (nm)
H
5.00 μM r(G4C2)2,0.00 μM TMPyP4
4.98 μM r(G4C2)2,1.99 μM TMPyP4
4.92 μM r(G4C2)2,7.87 μM TMPyP4
D.E. (mdeg/cm.M)
Wavelength (nm)

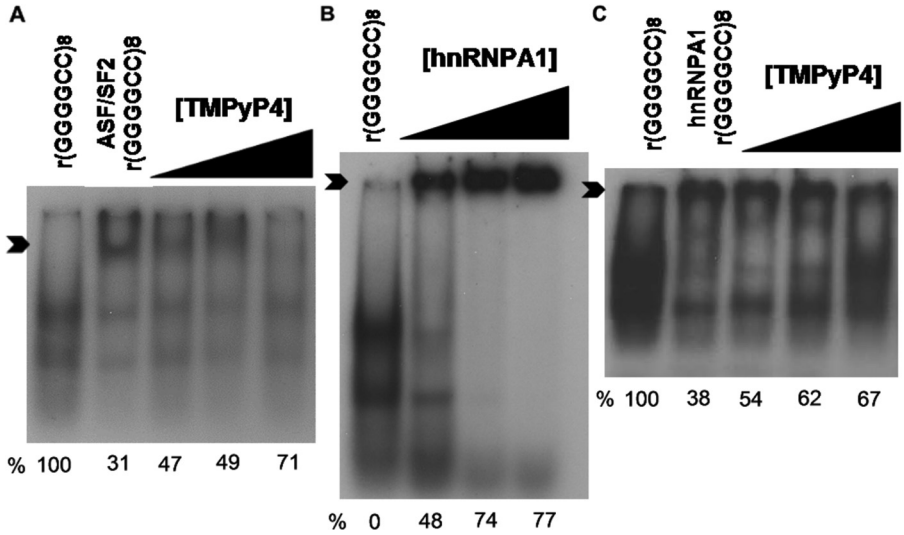

FIGURE 2. **The porphyrin TMPyP4 disrupts protein binding to the *C9orf72* RNA G-quadruplex.** *A*, migration of [γ-^{32}P]-labeled r(GGGGCC)$_8$ in the presence of 20 μM ASF/SF2 and 0, 10, 25, and 50 μM TMPyP4 electrophoresed on a 8% polyacrylamide gel. The amount of RNA bound by ASF/SF2 is 69% in the absence of TMPyP4, and the amount of protein-free RNA increased with increasing amounts of TMPyP4 (see %), as determined by densitometric analysis. *B*, migration of [γ-^{32}P]-labeled r(GGGGCC)$_8$ in the presence of 0, 7.5, 15, and 20 μM hnRNPA1. The amount of RNA bound increased with increasing amounts of hnRNPA1 (see %). *C*, migration of [γ-^{32}P]-labeled r(GGGGCC)$_8$ in the presence of 7.5 μM hnRNPA1 and 0, 10, 25, and 50 μM TMPyP4. The amount of RNA bound by hnRNPA1 is 62% in the absence of TMPyP4, and the amount of protein-free RNA increased with increasing amounts of TMPyP4 (see %), as determined by densitometric analysis. The ability of TMPyP4 to disrupt the interaction of protein binding was reproducible, and for hnRNPA1, it was statistically significant (Student's *t* test, $p = 0.032$).

increasing concentrations of TMPyP4, there was a disruption of ASF/SF2-RNA complexes exhibited by a loss in the band shift complex and an increase in the protein-free RNAs (Fig. 2*A*). Thus, TMPyP4 can interfere with ASF/SF2-r(GGGGCC)8 binding, providing proof of principle for disruption of potentially deleterious protein-RNA interactions.

To further test the potential of TMPyP4 to interfere with protein interaction, we assessed its effect upon the binding of hnRNPA1, an r(GGGGCC)*n*-binding protein that may have implications for ALS-FTD (6, 10). Previously, it was shown that hnRNPA1, or its proteolytic fragment UP1, could bind to various G-rich repeats, including telomeres and the fragile X-associated (CGG)*n* repeat (44–46). To test the potential interaction between hnRNPA1 and r(GGGGCC)8, a band shift assay was performed in the presence of increasing concentrations of purified hnRNPA1 (Fig. 2*B*). Binding of the r(GGGGCC)8 repeat to hnRNPA1 was evidenced by retention of the RNA-protein complexes in the well (Fig. 2*B*, *lanes 2–3*, see *arrowhead*), a phenomenon previously observed for the interaction of MBNL1 to r(CUG)*n* repeats (47, 48). Upon the addition of increasing amounts of TMPyP4, we observed a reduction in the intensity of the autoradiographic signal in the well and a coincident increase of protein-free RNA (Fig. 2*C*, *lanes 3–5*, see *arrowhead* and %). This is indicative of disruption of the hnRNPA1-r(GGGGCC)8 complex by TMPyP4. Thus, TMPyP4 is able to disrupt various protein-RNA complexes.

CONCLUSION

It has been shown that the formation of RNA foci and protein sequestration may be pathogenic in cases of ALS-FTD caused by expansion of the *C9orf72* repeat. Although point mutations in hnRNPA1 were previously shown to cause aggregation of hnRNPA1 in ALS-FTD patient brains (9) and non-mutant hnRNPA1 was independently shown to bind to r(GGGGCC)*n* repeats (6), the role of hnRNPA1 in a toxic RNA pathway is unknown. A potential role of ASF/SF2 in *C9orf72* expansion disease pathogenesis has been suggested by the presence of ASF/SF2 proteins in expanded r(GGGGCC)*n* RNA foci (9). If either hnRNPA1 or ASF/SF2 is involved in a toxic RNA pathway, the disruption of their interaction by small molecule ligands, such as TMPyP4, provides proof of principle that this is a viable avenue for the development of therapeutic treatments. Such an approach may complement RNA-directed antisense oligonucleotide attacks (49–51). The function of the G-quadruplex in RAN translation, although currently unknown, could also be modulated through its interaction with TMPyP4. However, there are currently no cellular assays to test the effect of TMPyP4 on RAN translation. The precise role of RNA structure in pathogenesis, splicing, or RAN translation of the *C9orf72* transcript remains to be determined; if the facile and extremely stable formation of a G-quadruplex by the r(GGGGCC)*n* repeat is involved, the perturbation of this

FIGURE 1. **The porphyrin TMPyP4 binds the *C9orf72* RNA G-quadruplex.** *A*, schematic of a G-quartet with 4 guanine residues interacting through Hoogsteen bonding (*dashed lines*). *B*, the structure of TMPyP4. *C*, a parallel-stranded G-quadruplex structure. *D*, migration of [γ-^{32}P]ATP end-labeled r(GGGGCC)$_8$ in the presence of 10, 25, 50, and 100 μM TMPyP4 in native 8% polyacrylamide gel. *E*, absorption titration of 15 μM TMPyP4 with (GGGGCC)$_8$ G-quadruplex in the presence of 100 mM KCl. *Inset*, the plot of α (fraction of bound porphyrin *versus* [RNA] concentration of RNA). All spectra were measured in 10 mM Tris-HCl (pH 7.5) and 0.1 mM EDTA at room temperature. *F*, CD titration of 5 μM r(GGGGCC)$_8$ with aliquots of 1 M TMPyP4 in the presence of 100 mM KCl, at 25 °C. *G*, CD titration of 5 μM r(GGGGCC)$_5$ with aliquots of 1 M TMPyP4 in the presence of 100 mM KCl, at 25 °C. *H*, CD titration of 5 μM r(GGGGCC)$_2$ with aliquots of 1 M TMPyP4 in the presence of 100 mM KCl, at 25 °C. *mdeg*, millidegrees; *D.E.*, $\delta\epsilon$.

structure by small molecule ligands may prove useful as a tool in understanding the role of RNA structure in these processes.

Acknowledgment—We thank Dr. Tigran Chalikian for use of UV and CD spectrophotometer.

REFERENCES

1. Turner, M. R., Hardiman, O., Benatar, M., Brooks, B. R., Chio, A., de Carvalho, M., Ince, P. G., Lin, C., Miller, R. G., Mitsumoto, H., Nicholson, G., Ravits, J., Shaw, P. J., Swash, M., Talbot, K., Traynor, B. J., Van den Berg, L. H., Veldink, J. H., Vucic, S., and Kiernan, M. C. (2013) Controversies and priorities in amyotrophic lateral sclerosis. *Lancet Neurol.* **12,** 310–322
2. DeJesus-Hernandez, M., Mackenzie, I. R., Boeve, B. F., Boxer, A. L., Baker, M., Rutherford, N. J., Nicholson, A. M., Finch, N. A., Flynn, H., Adamson, J., Kouri, N., Wojtas, A., Sengdy, P., Hsiung, G. Y., Karydas, A., Seeley, W. W., Josephs, K. A., Coppola, G., Geschwind, D. H., Wszolek, Z. K., Feldman, H., Knopman, D. S., Petersen, R. C., Miller, B. L., Dickson, D. W., Boylan, K. B., Graff-Radford, N. R., and Rademakers, R. (2011) Expanded GGGGCC hexanucleotide repeat in noncoding region of C9orf72 causes chromosome 9p-linked FTD and ALS. *Neuron* **72,** 245–256
3. Renton, A. E., Majounie, E., Waite, A., Simón-Sánchez, J., Rollinson, S., Gibbs, J. R., Schymick, J. C., Laaksovirta, H., van Swieten, J. C., Myllykangas, L., Kalimo, H., Paetau, A., Abramzon, Y., Remes, A. M., Kaganovich, A., Scholz, S. W., Duckworth, J., Ding, J., Harmer, D. W., Hernandez, D. G., Johnson, J. O., Mok, K., Ryten, M., Trabzuni, D., Guerreiro, R. J., Orrell, R. W., Neal, J., Murray, A., Pearson, J., Jansen, I. E., Sondervan, D., Seelaar, H., Blake, D., Young, K., Halliwell, N., Callister, J. B., Toulson, G., Richardson, A., Gerhard, A., Snowden, J., Mann, D., Neary, D., Nalls, M. A., Peuralinna, T., Jansson, L., Isoviita, V. M., Kaivorinne, A. L., Hölttä-Vuori, M., Ikonen, E., Sulkava, R., Benatar, M., Wuu, J., Chiò, A., Restagno, G., Borghero, G., Sabatelli, M., Heckerman, D., Rogaeva, E., Zinman, L., Rothstein, J. D., Sendtner, M., Drepper, C., Eichler, E. E., Alkan, C., Abdullaev, Z., Pack, S. D., Dutra, A., Pak, E., Hardy, J., Singleton, A., Williams, N. M., Heutink, P., Pickering-Brown, S., Morris, H. R., Tienari, P. J., and Traynor, B. J. (2011) A hexanucleotide repeat expansion in C9orf72 is the cause of chromosome 9p21-linked ALS-FTD. *Neuron* **72,** 257–268
4. Gómez-Tortosa, E., Gallego, J., Guerrero-López, R., Marcos, A., Gil-Neciga, E., Sainz, M. J., Díaz, A., Franco-Macías, E., Trujillo-Tiebas, M. J., Ayuso, C., and Pérez-Pérez, J. (2013) C9orf72 hexanucleotide expansions of 20–22 repeats are associated with frontotemporal deterioration. *Neurology* **80,** 366–370
5. Shin, J., Charizanis, K., and Swanson, M. S. (2009) Pathogenic RNAs in microsatellite expansion disease. *Neurosci. Lett.* **466,** 99–102
6. Mori, K., Lammich, S., Mackenzie, I. R., Forné, I., Zilow, S., Kretzschmar, H., Edbauer, D., Janssens, J., Kleinberger, G., Cruts, M., Herms, J., Neumann, M., Van Broeckhoven, C., Arzberger, T., and Haass, C. (2013) hnRNP A3 binds to GGGGCC repeats and is a constituent of p62-positive/TDP43-negative inclusions in the hippocampus of patients with *C9orf72* mutations. *Acta Neuropathol.* **125,** 413–423
7. Reddy, K., Zamiri, B., Stanley, S. Y., Macgregor, R. B., Jr., and Pearson, C. E. (2013) The disease-associated r(GGGGCC)*n* repeat from the *C9orf72* gene forms tract length-dependent uni- and multimolecular RNA G-quadruplex structures. *J. Biol. Chem.* **288,** 9860–9866
8. Xu, Z., Poidevin, M., Li, X., Li, Y., Shu, L., Nelson, D. L., Li, H., Hales, C. M., Gearing, M., Wingo, T. S., and Jin, P. (2013) Expanded GGGGCC repeat RNA associated with amyotrophic lateral sclerosis and frontotemporal dementia causes neurodegeneration. *Proc. Natl. Acad. Sci. U.S.A.* **110,** 7778–7783
9. Lee, Y. B., Chen, H. J., Peres, J. N., Gomez-Deza, J., Attig, J., Stalekar, M., Troakes, C., Nishimura, A. L., Scotter, E. L., Vance, C., Adachi, Y., Sardone, V., Miller, J. W., Smith, B. N., Gallo, J. M., Ule, J., Hirth, F., Rogelj, B., Houart, C., and Shaw, C. E. (2013) Hexanucleotide repeats in ALS/FTD form length-dependent RNA foci, sequester RNA binding proteins, and are neurotoxic. *Cell Rep.* **5,** 1178–1186
10. Kim, H. J., Kim, N. C., Wang, Y. D., Scarborough, E. A., Moore, J., Diaz, Z., MacLea, K. S., Freibaum, B., Li, S., Molliex, A., Kanagaraj, A. P., Carter, R., Boylan, K. B., Wojtas, A. M., Rademakers, R., Pinkus, J. L., Greenberg, S. A., Trojanowski, J. Q., Traynor, B. J., Smith, B. N., Topp, S., Gkazi, A. S., Miller, J., Shaw, C. E., Kottlors, M., Kirschner, J., Pestronk, A., Li, Y. R., Ford, A. F., Gitler, A. D., Benatar, M., King, O. D., Kimonis, V. E., Ross, E. D., Weihl, C. C., Shorter, J., and Taylor, J. P. (2013) Mutations in prion-like domains in hnRNPA2B1 and hnRNPA1 cause multisystem proteinopathy and ALS. *Nature* **495,** 467–473
11. Reddy, K., and Pearson, C. E. (2013) RAN rranslation: Fragile X in the running. *Neuron* **78,** 405–408
12. Ash, P. E., Bieniek, K. F., Gendron, T. F., Caulfield, T., Lin, W. L., Dejesus-Hernandez, M., van Blitterswijk, M. M., Jansen-West, K., Paul, J. W., 3rd, Rademakers, R., Boylan, K. B., Dickson, D. W., and Petrucelli, L. (2013) Unconventional translation of C9orf72 GGGGCC expansion generates insoluble polypeptides specific to c9FTD/ALS. *Neuron* **77,** 639–646
13. Zu, T., Liu, Y., Bañez-Coronel, M., Reid, T., Pletnikova, O., Lewis, J., Miller, T. M., Harms, M. B., Falchook, A. E., Subramony, S. H., Ostrow, L. W., Rothstein, J. D., Troncoso, J. C., and Ranum, L. P. (2013) RAN proteins and RNA foci from antisense transcripts in C9orf72 ALS and frontotemporal dementia. *Proc. Natl. Acad. Sci. U.S.A.* **110,** E4968-E4977
14. Mori, K., Arzberger, T., Grässer, F. A., Gijselinck, I., May, S., Rentzsch, K., Weng, S. M., Schludi, M. H., van der Zee, J., Cruts, M., Van Broeckhoven, C., Kremmer, E., Kretzschmar, H. A., Haass, C., and Edbauer, D. (2013) Bidirectional transcripts of the expanded *C9orf72* hexanucleotide repeat are translated into aggregating dipeptide repeat proteins. *Acta Neuropathol.* **126,** 881–893
15. Gendron, T. F., Bieniek, K. F., Zhang, Y. J., Jansen-West, K., Ash, P. E., Caulfield, T., Daughrity, L., Dunmore, J. H., Castanedes-Casey, M., Chew, J., Cosio, D. M., van Blitterswijk, M., Lee, W. C., Rademakers, R., Boylan, K. B., Dickson, D. W., and Petrucelli, L. (2013) Antisense transcripts of the expanded C9orf72 hexanucleotide repeat form nuclear RNA foci and undergo repeat-associated non-ATG translation in c9FTD/ALS. *Acta Neuropathol.* **126,** 829–844
16. Zu, T., Gibbens, B., Doty, N. S., Gomes-Pereira, M., Huguet, A., Stone, M. D., Margolis, J., Peterson, M., Markowski, T. W., Ingram, M. A., Nan, Z., Forster, C., Low, W. C., Schoser, B., Somia, N. V., Clark, H. B., Schmechel, S., Bitterman, P. B., Gourdon, G., Swanson, M. S., Moseley, M., and Ranum, L. P. (2011) Non-ATG-initiated translation directed by microsatellite expansions. *Proc. Natl. Acad. Sci. U.S.A.* **108,** 260–265
17. Pearson, C. E. (2011) Repeat associated non-ATG translation initiation: one DNA, two transcripts, seven reading frames, potentially nine toxic entities! *PLoS Genet.* **7,** e1002018
18. Wheeler, T. M., Sobczak, K., Lueck, J. D., Osborne, R. J., Lin, X., Dirksen, R. T., and Thornton, C. A. (2009) Reversal of RNA dominance by displacement of protein sequestered on triplet repeat RNA. *Science* **325,** 336–339
19. Fratta, P., Mizielinska, S., Nicoll, A. J., Zloh, M., Fisher, E. M., Parkinson, G., and Isaacs, A. M. (2012) *C9orf72* hexanucleotide repeat associated with amyotrophic lateral sclerosis and frontotemporal dementia forms RNA G-quadruplexes. *Sci. Rep.* **2,** 1016
20. Gellert, M., Lipsett, M. N., and Davies, D. R. (1962) Helix formation by guanylic acid. *Proc. Natl. Acad. Sci. U.S.A.* **48,** 2013–2018
21. Sen, D., and Gilbert, W. (1990) A sodium-potassium switch in the formation of four-stranded G4-DNA. *Nature* **344,** 410–414
22. Miura, T., Benevides, J. M., and Thomas, G. J., Jr. (1995) A phase diagram for sodium and potassium ion control of polymorphism in telomeric DNA. *J. Mol. Biol.* **248,** 233–238
23. Biffi, G., Tannahill, D., McCafferty, J., and Balasubramanian, S. (2013) Quantitative visualization of DNA G-quadruplex structures in human cells. *Nat. Chem.* **5,** 182–186
24. Xu, Y., and Komiyama, M. (2013) Evidence for G-quadruplex DNA in human cells. *Chembiochem* **14,** 927–928
25. Eddy, J., and Maizels, N. (2008) Conserved elements with potential to form polymorphic G-quadruplex structures in the first intron of human genes. *Nucleic Acids Res.* **36,** 1321–1333
26. Melko, M., and Bardoni, B. (2010) The role of G-quadruplex in RNA metabolism: involvement of FMRP and FMR2P. *Biochimie* **92,** 919–926
27. Darnell, J. C., Jensen, K. B., Jin, P., Brown, V., Warren, S. T., and Darnell, R. B. (2001) Fragile X mental retardation protein targets G quartet mRNAs

important for neuronal function. *Cell* **107,** 489–499
28. Brown, V., Jin, P., Ceman, S., Darnell, J. C., O'Donnell, W. T., Tenenbaum, S. A., Jin, X., Feng, Y., Wilkinson, K. D., Keene, J. D., Darnell, R. B., and Warren, S. T. (2001) Microarray identification of FMRP-associated brain mRNAs and altered mRNA translational profiles in fragile X syndrome. *Cell* **107,** 477–487
29. Bugaut, A., and Balasubramanian, S. (2012) 5′-UTR RNA G-quadruplexes: translation regulation and targeting. *Nucleic Acids Res.* **40,** 4727–4741
30. Subramanian, M., Rage, F., Tabet, R., Flatter, E., Mandel, J. L., and Moine, H. (2011) G-quadruplex RNA structure as a signal for neurite mRNA targeting. *EMBO Rep.* **12,** 697–704
31. Darnell, J. C., Warren, S. T., and Darnell, R. B. (2004) The fragile X mental retardation protein, FMRP, recognizes G-quartets. *Ment. Retard. Dev. Disabil. Res. Rev.* **10,** 49–52
32. Düchler, M. (2012) G-quadruplexes: targets and tools in anticancer drug design. *J. Drug Target* **20,** 389–400
33. Morris, M. J., Wingate, K. L., Silwal, J., Leeper, T. C., and Basu, S. (2012) The porphyrin TMPyP4 unfolds the extremely stable G-quadruplex in MT3-MMP mRNA and alleviates its repressive effect to enhance translation in eukaryotic cells. *Nucleic Acids Res.* **40,** 4137–4145
34. Weisman-Shomer, P., Cohen, E., Hershco, I., Khateb, S., Wolfovitz-Barchad, O., Hurley, L. H., and Fry, M. (2003) The cationic porphyrin TMPyP4 destabilizes the tetraplex form of the fragile X syndrome expanded sequence d(CGG)*n*. *Nucleic Acids Res.* **31,** 3963–3970
35. Ofer, N., Weisman-Shomer, P., Shklover, J., and Fry, M. (2009) The quadruplex r(CGG)*n* destabilizing cationic porphyrin TMPyP4 cooperates with hnRNPs to increase the translation efficiency of fragile X premutation mRNA. *Nucleic Acids Res.* **37,** 2712–2722
36. Oostra, B. A., and Willemsen, R. (2009) *FMR1*: a gene with three faces. *Biochim Biophys Acta* **1790,** 467–477
37. Cantor, C. R., Warshaw, M. M., and Shapiro, H. (1970) Oligonucleotide interactions. 3. Circular dichroism studies of the conformation of deoxyoligonucleotides. *Biopolymers* **9,** 1059–1077
38. Keating, L. R., and Szalai, V. A. (2004) Parallel-stranded guanine quadruplex interactions with a copper cationic porphyrin. *Biochemistry* **43,** 15891–15900
39. Wei, C., Wang, L., Jia, G., Zhou, J., Han, G., and Li, C. (2009) The binding mode of porphyrins with cation side arms to (TG4T)4 G-quadruplex: spectroscopic evidence. *Biophys. Chem.* **143,** 79–84
40. Balagurumoorthy, P., and Brahmachari, S. K. (1994) Structure and stability of human telomeric sequence. *J. Biol. Chem.* **269,** 21858–21869
41. Phan, A. T., Kuryavyi, V., and Patel, D. J. (2006) DNA architecture: from G to Z. *Curr. Opin. Struct. Biol.* **16,** 288–298
42. Martino, L., Pagano, B., Fotticchia, I., Neidle, S., and Giancola, C. (2009) Shedding light on the interaction between TMPyP4 and human telomeric quadruplexes. *J Phys Chem B* **113,** 14779–14786
43. Lane, A. N., Chaires, J. B., Gray, R. D., and Trent, J. O. (2008) Stability and kinetics of G-quadruplex structures. *Nucleic Acids Res.* **36,** 5482–5515
44. Zhang, Q. S., Manche, L., Xu, R. M., and Krainer, A. R. (2006) hnRNP A1 associates with telomere ends and stimulates telomerase activity. *RNA* **12,** 1116–1128
45. Flynn, R. L., Centore, R. C., O'Sullivan, R. J., Rai, R., Tse, A., Songyang, Z., Chang, S., Karlseder, J., and Zou, L. (2011) TERRA and hnRNPA1 orchestrate an RPA-to-POT1 switch on telomeric single-stranded DNA. *Nature* **471,** 532–536
46. Nakagama, H., Higuchi, K., Tanaka, E., Tsuchiya, N., Nakashima, K., Katahira, M., and Fukuda, H. (2006) Molecular mechanisms for maintenance of G-rich short tandem repeats capable of adopting G4 DNA structures. *Mutat. Res.* **598,** 120–131
47. Yuan, Y., Compton, S. A., Sobczak, K., Stenberg, M. G., Thornton, C. A., Griffith, J. D., and Swanson, M. S. (2007) Muscleblind-like 1 interacts with RNA hairpins in splicing target and pathogenic RNAs. *Nucleic Acids Res.* **35,** 5474–5486
48. Warf, M. B., and Berglund, J. A. (2007) MBNL binds similar RNA structures in the CUG repeats of myotonic dystrophy and its pre-mRNA substrate cardiac troponin T. *RNA* **13,** 2238–2251
49. Lagier-Tourenne, C., Baughn, M., Rigo, F., Sun, S., Liu, P., Li, H. R., Jiang, J., Watt, A. T., Chun, S., Katz, M., Qiu, J., Sun, Y., Ling, S. C., Zhu, Q., Polymenidou, M., Drenner, K., Artates, J. W., McAlonis-Downes, M., Markmiller, S., Hutt, K. R., Pizzo, D. P., Cady, J., Harms, M. B., Baloh, R. H., Vandenberg, S. R., Yeo, G. W., Fu, X. D., Bennett, C. F., Cleveland, D. W., and Ravits, J. (2013) Targeted degradation of sense and antisense *C9orf72* RNA foci as therapy for ALS and frontotemporal degeneration. *Proc. Natl. Acad. Sci. U.S.A.* **110,** E4530–E4539
50. Sareen, D., O'Rourke, J. G., Meera, P., Muhammad, A. K., Grant, S., Simpkinson, M., Bell, S., Carmona, S., Ornelas, L., Sahabian, A., Gendron, T., Petrucelli, L., Baughn, M., Ravits, J., Harms, M. B., Rigo, F., Bennett, C. F., Otis, T. S., Svendsen, C. N., and Baloh, R. H. (2013) Targeting RNA foci in iPSC-derived motor neurons from ALS patients with a C9orf72 repeat expansion. *Sci. Transl. Med.* **5,** 208ra149
51. Donnelly, C. J., Zhang, P. W., Pham, J. T., Heusler, A. R., Mistry, N. A., Vidensky, S., Daley, E. L., Poth, E. M., Hoover, B., Fines, D. M., Maragakis, N., Tienari, P. J., Petrucelli, L., Traynor, B. J., Wang, J., Rigo, F., Bennett, C. F., Blackshaw, S., Sattler, R., and Rothstein, J. D. (2013) RNA toxicity from the ALS/FTD C9orf72 expansion is mitigated by antisense intervention. *Neuron* **80,** 415–428